

An excitation theory for bound modes, leaky modes, and residual-wave currents on stripline structures

David R. Jackson,¹ Francisco Mesa,² Manuel J. Freire,² Dennis P. Nyquist,³ and Carlo Di Nallo⁴

Abstract. The nature of the current on a general multilayered printed-circuit stripline structure excited by a delta-gap source is investigated. The current is obtained through the construction of a semianalytical three-dimensional (3-D) Green's function, which accounts for the presence of the infinite conducting strip and the layered background structure. The 3-D Green's function is obtained by Fourier transforming the delta-gap source in the longitudinal (z) direction, which effectively resolves the 3-D problem of a delta-gap source into a superposition of 2-D problems, each of which is infinite in the z direction. The analysis allows for a convenient decomposition of the strip current into a sum of constituent parts. In particular, the strip current is first resolved into a set of bound-mode current waves and a continuous-spectrum current. The continuous-spectrum current is then represented as a set of physical leaky-mode currents in addition to a set of "residual-wave" currents, which arise from the steepest-descent integration paths. An asymptotic analysis reveals that the residual-wave currents decay algebraically as $z^{-3/2}$. Far away from the source, the residual-wave currents dominate the continuous-spectrum strip current. Results are shown for a specific type of stripline structure, but the analysis and conclusions are valid for arbitrary multilayer stripline structures.

1. Introduction

A practical source on a printed-circuit transmission line will excite a current on the line that consists of one or more bound (proper) modes, as well as a continuous-spectrum part. The continuous-spectrum part of the current accounts for radiation from the source on the printed-circuit line, in analogy with radiation from simple sources in dielectric layers where the continuous spectrum has been well characterized [Collin, 1960]. For structures that are open vertically, radiation may

occur into free space as well as into the background modes of the surrounding layered structure (the structure without the printed strip transmission line). For structures that are closed vertically on top and bottom by ground planes, such as stripline structures, radiation can only occur into the background modes of the structure, which are parallel-plate modes. The purpose of the present study is to explore the nature of the continuous-spectrum current on a printed-circuit line, confining the investigation to vertically closed stripline structures for simplicity. A delta-gap source on an infinite line will be used to represent a practical source, which launches the bound modes as well as the continuous-spectrum current on the line. A delta-gap source on an infinite stripline structure is shown in Figure 1. In Figure 1 a two-layered stripline structure (covered microstrip) is shown. This is a representative multilayer stripline structure that supports the existence of both bound and leaky modes. Results will be presented for this particular structure, although the analysis and conclusions will apply for an arbitrary multilayer stripline structure.

The primary tool used in the investigation of the strip current excited by the delta-gap source is a

¹Department of Electrical and Computer Engineering, University of Houston, Houston, Texas.

²Microwave Group, University of Seville, Seville, Spain.

³Department of Electrical Engineering, Michigan State University, East Lansing.

⁴Department of Electronic Engineering, University of Rome "La Sapienza," Rome, Italy.

semianalytical “three-dimensional (3-D) Green’s function” [Di Nallo *et al.*, 1998]. This 3-D Green’s function, as it is called, gives the current $I(z)$ on the strip due to the delta-gap excitation (this is a three-dimensional problem). The 3-D Green’s function is constructed by Fourier transforming the impressed source field of the delta-gap in the longitudinal (z) direction. This decomposes the 3-D problem with the delta-gap excitation into a superposition of 2-D problems, each corresponding to an infinite printed-circuit line with an infinite uniform phased source excitation. The 2-D problem is solved using a Galerkin moment method procedure in the spectral domain. The resulting 3-D Green’s function is in the form of an inverse Fourier transform, involving an integration in the spectral longitudinal wavenumber k_z . The integrand itself is defined in terms of a spectral integration in the transverse wavenumber k_x plane, arising from the solution of the corresponding 2-D problem. For a given value of k_z , different paths of integration in the complex k_x plane may be used to compute the integrand. This results in the integrand being a multivalued function of k_z . As established by Di Nallo *et al.* [1998], square-root-type branch cuts appear in the k_z plane at the locations $k_{zb} = \pm k_{pp}$, where k_{pp} is the wavenumber of a parallel-plate mode of the background structure. In addition to branch points, pole singularities occur in the k_z plane, corresponding to both bound (proper) modes and leaky modes. An understanding of the branch point and pole singularities of the integrand is very important for physically interpreting, classifying, and characterizing the current excited by the delta-gap source, which is the main subject of the present investigation.

To characterize the strip current, the original path of integration in the k_z plane is first deformed into a sum of two types of paths: one path that encircles all of the branch cuts, and a set of paths that encircle each of the bound-mode pole singularities. This leads to a decomposition of the total strip current into a set of bound-mode currents (from the pole residues) and a continuous-spectrum current (from the path that encircles the branch cuts) [Nyquist and Infante, 1995].

The latter component of the strip current corresponds to radiation. As will be shown, the path around the branch cuts can then be further deformed into a set of steepest-descent paths (SDPs) that encircle the branch points in the k_z plane, along with a set of paths that encircle the physical leaky-mode poles [Jackson *et al.*, 1998]. It will

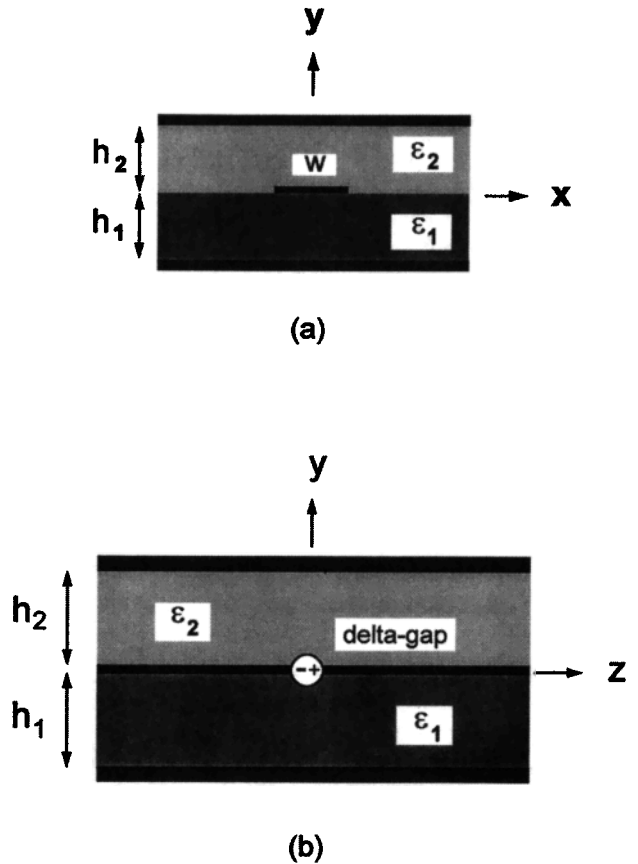


Figure 1. Geometry of the two-layer stripline (covered microstrip) structure, which is a representative multilayer stripline structure. Results will be presented for this particular structure.

thus be shown that the continuous-spectrum current can be represented as a set of physical leaky-mode currents plus a set of residual-wave currents, defined as the current contributions arising from the SDP integrations.

An asymptotic analysis of the residual-wave currents reveals that each one decays algebraically as $z^{-3/2}$ and propagates with a wavenumber k_{pp} , corresponding to the wavenumber of a parallel-plate waveguide mode. Physically, the residual-wave currents are interpreted as that part of the continuous-spectrum current that is not well represented by the leaky-mode currents. Far from the source, after the leaky-mode currents have decayed exponentially to a negligible value, the residual-wave currents will form the dominant part of the continuous-spectrum current on the line. Numerical results are presented that confirm the predicted asymptotic behavior of the current.

2. Calculation of Strip Current

For a delta-gap source on a printed-circuit line, such as the stripline structure shown in Figure 1, the current on the line, $I(z)$, is calculated in the form of an inverse Fourier transform involving a spectral integration in the longitudinal wavenumber k_z , as

$$I(z) = \frac{1}{2\pi} \int_{-\infty}^{\infty} \tilde{I}(k_z) e^{-jk_z z} dk_z. \quad (1)$$

The solution for the strip current begins by considering the electric field integral equation (EFIE) for the strip current. For simplicity, the current is assumed to be z directed (accurate for a narrow strip). The EFIE then has the form

$$E_z[J_z(x, z)] = P(x)L_g(z), \quad (2)$$

where $P(x)$ is a pulse function, defined as unity over the strip width, and $L_g(z)$ is a longitudinal profile function that describes the delta-gap source. Ideally, this longitudinal function is a delta function, although in practice it can be chosen as a narrow pulse function to accelerate the convergence of its transform. The current on the strip $J_z(x, z)$ is represented as

$$J_z(x, z) = I(z)\eta(x), \quad (3)$$

where $\eta(x)$ is a transverse shape (basis) function, normalized so that the integral across the strip width is unity (a convenient choice is a pulse function weighted by an edge-singularity term [Di Nallo *et al.*, 1998]). The assumption of a single basis function to represent the transverse shape of the current, as in (3), is accurate for a narrow strip. The formulation can be directly extended to allow for multiple basis functions, and x -directed current, although the formulation is limited here to a single basis function of longitudinal current for clarity. The effects of using multiple basis functions will be addressed later during the discussion of the asymptotic analysis and in the results section.

Inserting (3) into (2), and using the spectral domain Green's function to calculate the field, gives the result

$$\frac{1}{(2\pi)^2} \iint_{-\infty}^{\infty} \tilde{G}_z(k_x, k_z) \tilde{\eta}(k_x) \tilde{I}(k_z) e^{-j(k_x x + k_z z)} dk_x dk_z \quad (4)$$

$$= P(x)L_g(z).$$

The Fourier transform of the strip current, $\tilde{I}(k_z)$, is

found from enforcing this electric field integral equation over the strip width using $\eta(x)$ as a testing function, and then Fourier transforming the resulting equation (which is only a function of z) in z . The result is [Di Nallo *et al.*, 1998]

$$\tilde{I}(k_z) = \frac{2\pi \tilde{L}_g(k_z)}{\int_{-\infty}^{\infty} \tilde{\eta}^2(k_x) \tilde{G}_z(k_x, k_z) dk_x}. \quad (5)$$

The transform of the current is seen to involve a spectral integration in the transverse wavenumber (k_x) plane.

The inverse transform integration in the k_x plane in (1) is defined on a Riemann surface that has an infinite number of two-sheeted branch points, with each branch point k_{zb} corresponding to the propagation wavenumber of a parallel-plate mode of the background structure. The multivalued nature of the integrand function $\tilde{I}(k_x)$ is a consequence of the fact that different integration paths are possible in the evaluation of the denominator in (5); the paths may be deformed to go above or below the poles of the spectral domain Green's function at $k_{zp} = (k_{pp}^2 - k_z^2)^{1/2}$. For example, if a point in the k_x plane is on the bottom sheet of the branch point at $k_{zb} = k_{TM0}$, the corresponding k_x integration in (2) is along a path that detours around the TM_0 poles of $\tilde{G}_z(k_x, k_z)$ in the k_x plane; if k_z is on the top sheet, the path in the k_x plane does not detour around the TM_0 poles (it remains on the real axis of the k_x plane). A detailed discussion of the branch points is given by Di Nallo *et al.* [1998], and therefore further details are omitted here.

Figure 2a shows the k_x plane assuming that two parallel-plate waveguide modes (TM_0 and TE_1) are above cutoff, corresponding to two branch points along the real axis (an infinite number of branch points, corresponding to the higher-order parallel-plate modes, are on the imaginary axis). Figure 2a also shows the presence of bound-mode poles on the real axis, which are located to the right (left) of all branch points on the positive (negative) real axis (since the propagation wavenumber of a bound mode is greater than that of all parallel-plate modes of the background structure).

The inverse transform integration in the k_x plane of (1) is performed originally along path C in Figure 2a, on the top sheet with respect to all of the branch points, so that the spectral representation of $I(z)$ is in terms of waves that are proper (bound transversely). Path C (or

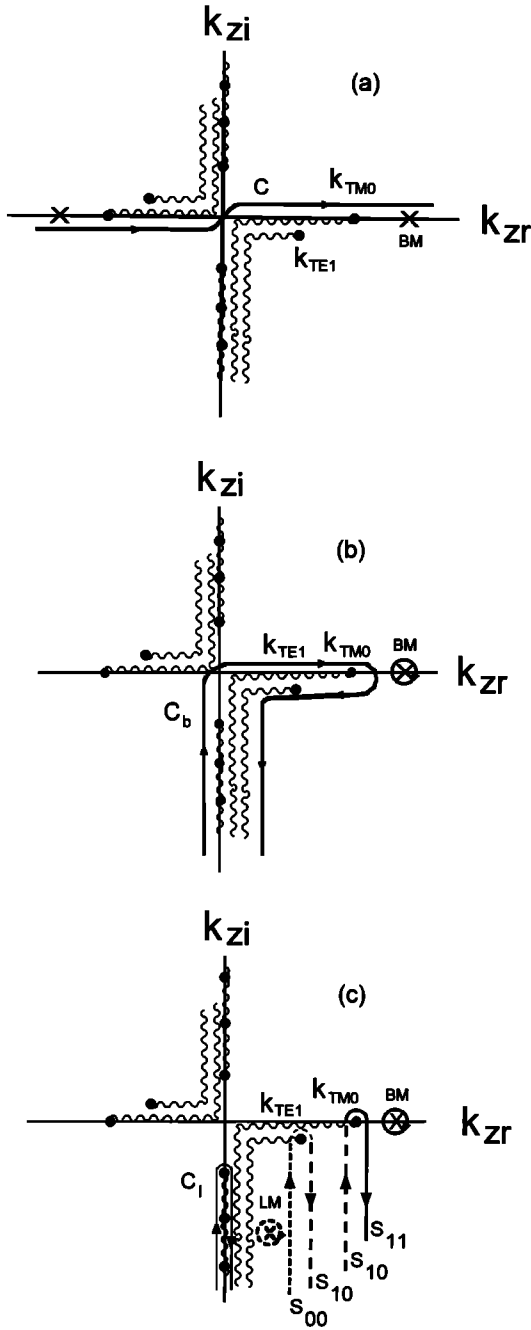


Figure 2. Paths of integration in the complex k_z (inverse Fourier transform) plane. (a) The original path of integration is shown, along with the bound-mode poles and the branch cuts. (b) The original path has been deformed into a path around all of the branch points and a residue contribution from the bound-mode poles. (c) The path around the branch points has been further deformed into a set of vertical steepest-descent paths that surround the branch points on the real axis, along with residue contributions from the physical leaky-mode poles.

one that is equivalent to it, by Cauchy's theorem) is convenient for numerical evaluation of the integral in (1) to calculate the total strip current. However, physical insight into the nature of the current is obtained by deforming the path. The path may first be deformed into a path C_b that goes around all of the branch points and a set of residue contributions from paths that encircle all of the bound-mode poles on the real axis, as shown in Figure 2b. The residue contributions from the bound-mode poles determine the launching amplitudes of the bound-mode currents on the printed-circuit line. The contribution from path C_b defines the continuous-spectrum current, which is responsible for radiation into the parallel-plate modes. The total current is thus represented as

$$I(z) = \frac{1}{2\pi} \int_{C_b} \tilde{I}(k_z) e^{-jk_z z} dk_z - j \sum_{N_b} \text{Res} \tilde{I}(k_z) e^{-jk_z z}, \quad (6)$$

where N_b is the number of propagating bound modes.

The first term in (6), representing the continuous-spectrum current, may be further decomposed by deformation of path C_b . During this deformation the left side of the path is first swept around the branch points on the imaginary axis and then past all of the branch points on the real axis except the rightmost one. The right side of path C_b is deformed to a vertical path that descends vertically from the rightmost branch point. The result is that path C_b is equivalent to a set of vertical paths, shown in Figure 2c (where the assumption is made that two parallel-plate modes are above cutoff, for simplicity). One path surrounds all of the branch points on the imaginary axis and is labeled path C_1 . This path remains entirely on the top sheet of all the branch points (as for path C_b). The remaining paths each encircle one corresponding branch point on the real axis. For each of these paths the left (ascending) side of the path is on the lower sheet of the corresponding branch point and all branch points to the right of the path. The right (descending) side of each path is on the top sheet of the corresponding branch point but is on the lower sheet of all branch points to the right of the path. The right side of the rightmost path is on the top sheet of all branch points. The notation S_{ij} ($i, j = 0, 1$) in Figure 2c denotes that the corresponding part of the path is on sheet i of the TE_1 branch point and sheet j of the TM_0 branch point, with 0 and 1 corresponding to the bottom and top sheets, respectively. The paths lie on the top sheet of all other branch points (the ones located on the imaginary axis). The reason for choosing vertical paths that surround the

branch points is that these correspond to SDPs, along which the exponential term $\exp(-jk_z z)$ in (6) decays as rapidly as possible. These SDP paths are analogous to the SDP paths that are used to evaluate the far field from sources inside layered media [Chew, 1990], in the limiting case when the observation point is located along the media interface. This choice of path will facilitate the asymptotic evaluation of these path contributions and will allow for a convenient representation of the continuous-spectrum current.

During the deformation of path C_b to the SDPs, one or more leaky-mode poles may be captured, depending on which sheets of the Riemann surface they lie. The leaky-mode poles are only captured if they lie on a combination of sheets that places them "close" to the original real-axis path (which is on the top sheet of all branch points), in the Riemann-surface sense. For example, in Figure 2c leaky-mode poles in the region $0 < \text{Re}(k_z) < k_{\text{TE}_1}$ are only captured if they lie on the bottom sheet of both branch points TE_1 and TM_0 . Leaky-mode poles in the region $k_{\text{TE}_1} < \text{Re}(k_z) < k_{\text{TM}_0}$ are only captured if they lie on the top sheet of branch point TE_1 and the bottom sheet of branch point TM_0 . Leaky-mode poles in the region $\text{Re}(k_z) > k_{\text{TM}_0}$ are never captured. The closeness of a leaky-mode pole to the real axis was used by *Di Nallo et al.* [1998] to establish a necessary condition for the corresponding leaky mode to be physically significant. As was also discussed by *Di Nallo et al.* [1998], the closeness condition is equivalent to the so-called path consistency condition for determining physical significance. This condition states that in order for a leaky mode to have physical significance, the path of integration in the k_x plane used to solve for the wavenumber k_{z_0} of the leaky mode must be consistent with the value of the phase constant $\beta = \text{Re}(k_{z_0})$ that is obtained from using that path. The path consistency condition was originally introduced [Nghiem et al., 1993] (called there the "condition of leakage") as a heuristic means of determining the physical significance of a leaky mode, based only on the 2-D analysis of an infinite line (with no source present). Although the closeness condition discussed by *Di Nallo et al.* [1998] provides a more substantive justification of when leaky modes are physically significant, the capturing of a leaky-mode pole by the steepest-descent path deformation provides the most rigorous means for establishing physical significance, as will be explained in the next section.

The current contributions from the SDPs are termed "residual-wave" currents. With this terminology the

continuous-spectrum current is decomposed into a set of all physical leaky-mode currents (corresponding to the leaky-mode poles that are captured by the deformation to the SDP paths) and a set of residual-wave currents, one for each background parallel-plate mode that is above cutoff (corresponding to a branch point on the real axis). Mathematically, the total strip current is then represented as

$$I(z) = \frac{1}{2\pi} \int_{C_I} \tilde{I}(k_z) e^{-jk_z z} dk_z - j \sum_{N_{lm}} \text{Res} \tilde{I}(k_{zp}) e^{-jk_{zp} z} + \sum_{N_{pp}} \frac{1}{2\pi} \int_{\text{SDP}_i} \tilde{I}(k_z) e^{-jk_z z} dk_z - j \sum_{N_b} \text{Res} \tilde{I}(k_{zp}) e^{-jk_{zp} z}. \quad (7)$$

The first term on the right-hand side of (7), from path C_I , corresponds to a current that decays exponentially very rapidly, since the path encloses branch points that are on the negative imaginary axis. It is essentially an evanescent higher-order mode near-field term that only exists very close to the source. The rate of decay of this current is determined by the branch point closest to the real axis, corresponding to the higher-order (evanescent) parallel-plate mode that is closest to cutoff. The second term is the set of currents coming from all physical leaky modes, with N_{lm} denoting the total number. The third term is the set of residual-wave currents, the total number of current waves being equal to the number of parallel-plate background modes above cutoff, denoted as N_{pp} . Finally, the last term is the set of bound-mode currents, with N_b denoting the total number of bound modes.

The leaky-mode currents decay exponentially with distance z , due to the complex propagation constants k_{zp} . At large distances from the source the current on the strip will be dominated by the bound-mode currents (which do not decay with distance for a lossless structure) and the residual-wave currents. The nature of the residual-wave currents will be established by an asymptotic analysis, given in the next section. This analysis reveals that the residual-wave currents decay algebraically with distance, rather than exponentially.

The definitions of leaky-mode and residual-wave currents given above provide a simple and convenient manner with which to classify the constituent parts of the continuous-spectrum current. The physical interpretation of the two constituent components, the leaky-mode currents and the residual-wave currents, is fairly straightforward when the leaky-mode poles are well within the physical regions of the k_z plane. In this

case, the residue contributions from the leaky-mode poles correspond to the currents of the physical leaky modes that are launched by the source. The residual-wave currents correspond to that part of the continuous-spectrum current that is not well approximated by the leaky-mode currents. Loosely speaking, the residual-wave currents may be thought of as a direct radiation from the source into the parallel-plate modes of the background structure, propagating in the direction of the strip.

When a leaky-mode pole is close to one of the SDP paths, and hence close to the boundary of the physical region, a physical interpretation of the leaky-mode and residual-wave currents becomes more ambiguous. As a leaky-mode pole approaches an SDP path, the leaky-mode current predicted by the corresponding pole residue loses correlation with the actual current spectrum on the line [Di Nallo *et al.*, 1998]. Furthermore, the leaky-mode current, as defined, is discontinuous as a leaky-mode pole crosses an SDP path (a pole goes from being captured to not captured). The residual-wave current is also discontinuous by an equal and opposite amount, so that the continuous-spectrum current remains continuous. In this transition region near an SDP boundary the physical interpretation of the leaky-mode and residual-wave currents is not clear. However, the mathematical calculations of the currents, as well as the asymptotic analysis presented in the next section, remain valid.

3. Asymptotic Evaluation of the Residual Wave Currents

3.1. Derivation of General Asymptotic Form

The residual-wave currents arise from the SDP integrations shown in Figure 2c, with one residual wave corresponding to each branch point on the real axis, which in turn corresponds to a parallel-plate mode above cutoff. To illustrate the asymptotic derivation, consider the residual wave corresponding to the TM_0 branch point. The residual wave has the form

$$I_{\text{Res}}(z) = \frac{1}{2\pi} \int_{\text{SDP}} \tilde{I}(k_z) e^{-jk_z z} dk_z, \quad (8)$$

where SDP is the vertical steepest-descent path surrounding the TM_0 branch point. On the left side of the SDP the path is on the top sheet of the TE_1 branch point but on the bottom sheet of the TM_0 branch point. The notation $\tilde{I}_{10}(k_z)$ is used to denote the function

$\tilde{I}(k_z)$ evaluated at this location on the Riemann surface, where the subscript 1 denotes top sheet and 0 denotes bottom sheet, in the order TE_1 , TM_0 . Similarly, the notation $\tilde{I}_{11}(k_z)$ denotes the value of the function on the right side of the SDP, which is located on the top sheet of both branch points. Both sides of the SDP path remain on the top sheet of the branch points located on the imaginary axis, and hence no subscript designation is needed for these branch points.

The change of variables

$$k_z = k_{TM_0} - js \quad (9)$$

allows the residual-wave current to be expressed as

$$I_{\text{Res}}(z) = e^{-jk_{TM_0}z} \int_0^{\infty} F(s) e^{-sz} ds, \quad (10)$$

where

$$F(s) = \frac{-j}{2\pi} [\tilde{I}_{11}(k_{TM_0} - js) - \tilde{I}_{10}(k_{TM_0} - js)]. \quad (11)$$

To asymptotically evaluate (10), Watson's lemma is invoked [Bleistein and Handelsman, 1975]. Watson's lemma allows the asymptotic behavior of the integral in (10) as $z \rightarrow \infty$ to be directly determined if the asymptotic behavior of $F(s)$ as $s \rightarrow 0$ is known. In particular, if it is known that

$$F(s) \approx As^\alpha \quad s \rightarrow 0, \quad (12)$$

Watson's lemma states that the asymptotic form for the integral in (10) may be determined by directly substituting (12) into the integral and performing the integration. Using the change of variables $t = sz$ yields the result

$$\int_0^{\infty} F(s) e^{-sz} ds \approx \frac{A}{z^{\alpha+1}} \int_0^{\infty} t^\alpha e^{-t} dt. \quad (13)$$

The integral in (13) is recognized as the integral form of the Gamma function [Abramowitz and Stegun, 1972], so that

$$\int_0^{\infty} F(s) e^{-sz} ds \approx \frac{A}{z^{\alpha+1}} \Gamma(\alpha+1). \quad (14)$$

The residual wave associated with the TM_0 parallel-plate mode then has the asymptotic form

$$I_{\text{Res}}(z) \approx A \Gamma(\alpha+1) \left[\frac{e^{-jk_{TM_0}z}}{z^{\alpha+1}} \right]. \quad (15)$$

This result shows that the residual-wave current decays algebraically (not exponentially, like the leaky-mode currents), but the amplitude A and the algebraic factor α remain to be determined. A determination of these constants requires consideration of the properties of the spectral domain Green's function $\tilde{G}_z(k_x, k_z)$ appearing in (5). The exact form of the spectral domain Green's function cannot be determined until the geometry of the layered structure has been specified (the number of layers, the layer thicknesses and permittivities, and the location of the strip conductor). In spite of this, it is possible to determine the asymptotic behavior of the spectral domain Green's function as $s \rightarrow 0$ in the general case, with the results holding for an arbitrary layered structure. Such an analysis is carried out below. The results show that $\alpha = 1/2$, so that the TM_0 residual-wave current behaves in general as

$$I_{\text{Res}}(z) \approx A \Gamma\left(\frac{3}{2}\right) \left[\frac{e^{-jk_{\text{TM}_0} z}}{z^{3/2}} \right], \quad (16)$$

for any type of layered stripline structure, when excited by a delta-gap source. A similar equation holds for the residual waves corresponding to the other parallel-plate modes, with the wavenumber k_{TM_0} replaced by the wavenumber of the corresponding parallel-plate mode, and the amplitude factor A different for each residual-wave current.

As noted in the previous section, the residual-wave current is discontinuous when a leaky-mode pole crosses the SDP path in the k_z plane. However, the asymptotic evaluation of the residual-wave current, given by (16), is always a continuous function of pole location. Physically, this means that the residual-wave current far from the source remains nearly continuous as the pole crosses the SDP boundary, since the discontinuity effect is negligible. Near to the source the discontinuity in the residual-wave current may be much more pronounced as the pole crosses the SDP boundary.

3.2 Calculation of Amplitude and Algebraic Decay Factors

The function $\tilde{I}(k_z)$ in (5) needs to be asymptotically approximated as $s \rightarrow 0$, corresponding to $k_z \rightarrow k_{\text{TM}_0}$ (illustrating once again for the TM_0 residual-wave current). The spectral domain Green's function $\tilde{G}_z(k_x, k_z)$ has poles at $k_{xp} = (k_{\text{TM}_0}^2 - k_z^2)^{1/2}$, which play a key role in the asymptotic evaluation. The term

$\tilde{I}_{11}(k_z)$ in (11) corresponds to the evaluation of the integral in the denominator of (5) by using a real-axis path of integration in the k_x plane, labeled as path C_{11} in Figure 3. The term $\tilde{I}_{10}(k_z)$, which is evaluated on the lower sheet of the branch point k_{TM_0} in the k_z plane, corresponds to a path of integration in the k_x plane that detours around the TM_0 poles of the spectral domain Green's function, as shown in Figure 3. Using (5) and (11), the function $F(s)$ can be written in terms of path integrals in the k_x plane as

$$F(s) = -j \tilde{L}_g(k_z) \left[\frac{1}{C_{11}} \int \tilde{\eta}^2(k_x) \tilde{G}_z(k_x, k_z) dk_x - \frac{1}{C_{10}} \int \tilde{\eta}^2(k_x) \tilde{G}_z(k_x, k_z) dk_x \right] \\ = -j \tilde{L}_g(k_z) \left[\frac{\int_{C_{10}} \tilde{\eta}^2(k_x) \tilde{G}_z(k_x, k_z) dk_x - \int_{C_{11}} \tilde{\eta}^2(k_x) \tilde{G}_z(k_x, k_z) dk_x}{\int_{C_{11}} \tilde{\eta}^2(k_x) \tilde{G}_z(k_x, k_z) dk_x + \int_{C_{10}} \tilde{\eta}^2(k_x) \tilde{G}_z(k_x, k_z) dk_x} \right]. \quad (17)$$

The numerator in (17) is equivalent to a contour integration around the TM_0 poles in the k_x plane, so that

$$\int_{C_{10}} \tilde{\eta}^2(k_x) \tilde{G}_z(k_x, k_z) dk_x - \int_{C_{11}} \tilde{\eta}^2(k_x) \tilde{G}_z(k_x, k_z) dk_x = \\ -2\pi j \tilde{\eta}^2(k_{xp}) \text{Res} \tilde{G}_z(k_{xp}, k_z) \\ + 2\pi j \tilde{\eta}^2(-k_{xp}) \text{Res} \tilde{G}_z(-k_{xp}, k_z), \quad (18)$$

where k_{xp} now refers to the pole in the first quadrant of the k_x plane. The residue at the pole location $-k_{xp}$ in the third quadrant can be related to the residue at k_{xp} in the first quadrant by noting that the pole behavior of the spectral domain Green's function is of the form

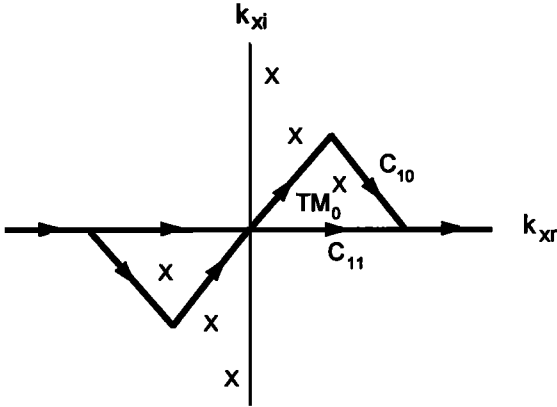


Figure 3. The k_x plane of integration, showing two possible paths, corresponding to the location of the point k_z on two different sheets of the Riemann surface. Path C_{11} stays on the real axis, while path C_{10} detours around the TM_0 poles of the spectral domain Green's function.

$$\tilde{G}_z^{\text{pole}}(k_x, k_z) = \frac{A_2}{k_x^2 - k_{xp}^2}. \quad (19)$$

From this equation it is easily established that the residue at $-k_{xp}$ is the negative of the residue at $+k_{xp}$. Also, the function $\eta(x)$ is assumed to be an even function, which implies that $\tilde{\eta}(k_x)$ is an even function as well. Hence (18) becomes

$$\int_{C_{10}} \tilde{\eta}^2(k_x) \tilde{G}_z(k_x, k_z) dk_x - \int_{C_{11}} \tilde{\eta}^2(k_x) \tilde{G}_z(k_x, k_z) dk_x = -4\pi j \tilde{\eta}^2(k_{xp}) \text{Res} \tilde{G}_z(k_{xp}, k_z). \quad (20)$$

The denominator in (17) cannot be evaluated exactly in closed form, but it can be analytically approximated in the limit of $s \rightarrow 0$. First, it is recognized that in this limit the pole locations in the k_x plane can be approximated from $k_{xp} = \left(k_{TM_0}^2 - (k_{TM_0} - js)^2 \right)^{1/2}$ as

$$k_{xp} \approx \pm \sqrt{2k_{TM_0}^2} e^{j\pi/4} \sqrt{s}. \quad (21)$$

Hence, as $s \rightarrow 0$ the poles are approaching the origin in the k_x plane along a 45° line. Because the poles are approaching the origin, the residues of the poles in the k_x plane are approaching infinity. To see this more clearly, the residue of the poles in the k_x plane is first related to the residue of the spectral domain Green's function in the transverse wavenumber (k_z) plane (in

the k_z plane the pole location $k_{zp} = k_{pp} = k_{TM_0}$ is a fixed number, which does not vary with k_z). Near the pole location in the k_z plane the spectral domain Green's function is approximated as

$$\tilde{G}_z(k_x, k_z) \approx \frac{A_1}{\Delta(k_z)} = \frac{A_1}{\Delta(\sqrt{k_x^2 + k_z^2})} \quad (22)$$

for some constant A_1 . The denominator term $\Delta(k_z)$ is zero at the pole location k_{zp} in the k_z plane, corresponding to k_{zp} in the k_z plane. The residue in the k_x plane is then written as

$$\begin{aligned} \text{Res} \tilde{G}_z(k_{xp}) &= \frac{A_1}{\Delta'(k_x)} \\ &= \frac{A_1}{\Delta'(k_z)} \frac{dk_z}{dk_x} \bigg|_{k_{xp}} \\ &= \frac{A_1}{\Delta'(k_z)} \frac{k_{zp}}{k_{xp}} \\ &= \text{Res} \tilde{G}_z(k_{zp}) \frac{k_{zp}}{k_{xp}}. \end{aligned} \quad (23)$$

The residue of the pole in the k_x plane is thus related to the residue in the k_z plane by a factor that clearly tends to infinity as $k_{xp} \rightarrow 0$, which happens when $s \rightarrow 0$, from (21).

Next, the integrals appearing in the denominator of (17) are expressed in terms of residue contributions by closing the paths along a large semicircle in the lower half plane. The results are

$$\begin{aligned} \int_{C_{10}} \tilde{\eta}^2(k_x) \tilde{G}_z(k_x, k_z) dk_x &= \\ &= -2\pi j \tilde{\eta}^2(k_{xp}) \text{Res} \tilde{G}_z(k_{xp}, k_z) + Q(k_z) \end{aligned} \quad (24)$$

$$\begin{aligned} \int_{C_{11}} \tilde{\eta}^2(k_x) \tilde{G}_z(k_x, k_z) dk_x &= \\ &= -2\pi j \tilde{\eta}^2(-k_{xp}) \text{Res} \tilde{G}_z(-k_{xp}, k_z) + Q(k_z) \end{aligned} \quad (25)$$

where k_{xp} now refers to the pole in the first quadrant of the k_x plane and the function $Q(k_z)$ is the residue

contribution from all of the poles on the negative imaginary axis in the k_x plane. (The locations of the poles corresponding to the higher-order parallel-plate modes are approximately on the imaginary axis, for small s .) It is assumed that the $Q(k_x)$ function remains finite as $k_x \rightarrow k_{TM_0}$, since none of the poles on the imaginary axis are approaching the origin. Hence this function can be neglected in the asymptotic limit. Then using once again the relation between the residues at k_{xp} and $-k_{xp}$, and the even property of the $\tilde{\eta}(k_x)$ function, the denominator term in (17) is approximated by

$$\int_{C_{11}} \tilde{\eta}^2(k_x) \tilde{G}_{zz}(k_x, k_z) dk_x \int_{C_{10}} \tilde{\eta}^2(k_x) \tilde{G}_{zz}(k_x, k_z) dk_x \quad (26)$$

$$\approx 4\pi^2 \tilde{\eta}^4(k_x) \text{Res}^2 \tilde{G}_{zz}(k_{xp}, k_z).$$

The approximation to (17) then becomes

$$F(s) \approx -\frac{\tilde{L}_g(k_z)}{\pi \tilde{\eta}^2(k_{xp})} \frac{1}{\text{Res} \tilde{G}_{zz}(k_{ip})} \left(\frac{k_{xp}}{k_{ip}} \right). \quad (27)$$

As $s \rightarrow 0$, the asymptotic form for $F(s)$ is directly obtained from (27), using (21) to approximate the k_{xp} term. This yields the result shown in (12) with $\alpha = 1/2$ and

$$A = -\frac{\sqrt{2}}{\pi} \tilde{L}_g(k_{TM_0}) \frac{1}{\tilde{\eta}^2(0)} \frac{1}{\sqrt{k_{TM_0}}} \frac{1}{\text{Res} \tilde{G}_{zz}(k_{TM_0})} e^{j\pi/4}. \quad (28)$$

The term $\tilde{\eta}^2(0)$ in (28) is unity, since the function $\eta(x)$ was normalized to correspond to a unity strip current. (Therefore it is interesting to note that the above result for the amplitude factor A is independent of the shape of the basis function that is assumed.) Furthermore, under the assumption of a delta-gap excitation, the term $\tilde{L}_g(k_{TM_0})$ is also unity. The only terms in (28) that must be determined numerically are the propagation wavenumber of the parallel-plate mode, k_{TM_0} , and the residue term. For layered stripline structures involving only a few layers, it is possible to calculate the residue term analytically. For general structures, this term may be computed by numerically integrating around the pole in the k_x plane, using Cauchy's theorem [Churchill, 1960].

4. Discussion

From the previous sections it is concluded that the current excited by a delta-gap source on a stripline structure consists of a set of bound-mode currents and a continuous-spectrum current. The continuous-spectrum current in turn consists of a set of physical leaky-mode currents and a set of residual-wave currents, with one residual-wave current corresponding to each parallel-plate mode of the background structure that is above cutoff. (In most practical cases, only the TM_0 mode will be above cutoff, in which case there is only one residual-wave current). Mathematically, the forms of the bound-mode current, leaky-mode current, and residual-wave current (illustrating with the TM_0 mode residual wave) are

$$I_{BM}(z) = A_{BM} e^{-j\beta_{BM} z}, \quad (29)$$

$$I_{LM}(z) = A_{LM} e^{-j\beta_{LM} z} e^{-\alpha_{LM} z}, \quad (30)$$

and

$$I_{RW}(z) = A_{RW} \left(\frac{1}{(k_{TM_0} z)^{3/2}} \right) e^{-jk_{TM_0} z}, \quad (31)$$

respectively, where

$$A_{RW} = A\Gamma(3/2)k_{TM_0}^{3/2}. \quad (32)$$

The bound modes do not decay with distance from the source (for a lossless structure), while the leaky-mode currents decay exponentially with an attenuation constant that depends on the location of the leaky-mode poles in the k_x plane, i.e., $\alpha_{LM} = -\text{Im}(k_{xp}^{LM})$. The residual-wave currents each propagate with a wavenumber equal to that of the corresponding parallel-plate mode of the background structure, and they decay as $z^{-3/2}$. Far away from the source the bound-mode and residual-wave currents will dominate (and extremely far from the source, only the bound-mode currents will remain). Assuming a single TM_0 residual-wave current, the distance z_0 at which a particular leaky-mode current begins to become negligible compared with the residual-wave current may be found by equating (30) and (31). This yields the transcendental equation

$$e^{-x} x^{3/2} = \left| \frac{A_{RW}}{A_{LM}} \left(\frac{\alpha}{k_{TM_0}} \right) \right|^{3/2}, \quad (33)$$

where $x = \alpha_{LM} z_0$. For a small attenuation constant and a

sufficiently large amplitude of excitation, a physical leaky-mode current may dominate the residual-wave current out to a relatively large distance, in which case the fields near the guiding structure may resemble those of the leaky mode. Eventually, however, the residual-wave current will dominate the continuous-spectrum current.

Physically, the residual-wave currents are that part of the continuous-spectrum current that is not well represented by the leaky-mode currents. The residual-wave currents may be thought of as a type of direct radiation from the delta-gap source in the form of parallel-plate modes. Ordinarily, an isolated source in a layered stripline structure will excite a cylindrically propagating parallel-plate mode with an amplitude that decays as $r^{-1/2}$ (this is expected from conservation of energy). It is interesting to note that the presence of the infinite conducting strip modifies the propagating parallel-plate mode so that the strip current decays as $z^{-3/2}$, with a faster decay than might otherwise be expected. The nature of the fields associated with the residual-wave current is a more complicated issue, which is presently under investigation.

As noted in the previous section, the physical interpretation of the leaky-mode and residual-wave currents becomes more ambiguous when a leaky-mode pole is close to a SDP path. Although the residual-wave

current will still behave asymptotically as predicted in such a transition region, the presence of a pole near the SDP may cause the residual-wave current to contain a nonnegligible contribution from the influence of the nearby pole. This exponentially decaying current will eventually die out, revealing the algebraic nature of the residual wave. In such a transition region, however, the physical distinction between the leaky-mode current and the residual-wave current is not clear, since the residual-wave current may contain an exponentially decaying component that is equal (or nearly equal) in magnitude to that of the leaky-mode current.

An interesting aspect of the asymptotic analysis is the consideration of the effects of including high-order basis functions in the analysis (recall that equation (3) assumed a single basis function $\eta(x)$ to represent the transverse current profile). To generalize the analysis, a more complete moment-method formulation has been carried out, using higher-order basis functions consisting of Chebyshev polynomials of the first and second kind weighted by an edge-singularity term [Mesa and Marqués, 1995]. Surprisingly, the inclusion of the higher-order basis functions did not improve the asymptotic accuracy of the residual-wave current calculation, i.e., the accuracy of the residual-wave current for large distances from the source. To explain this, consider that the asymptotic analysis is performed

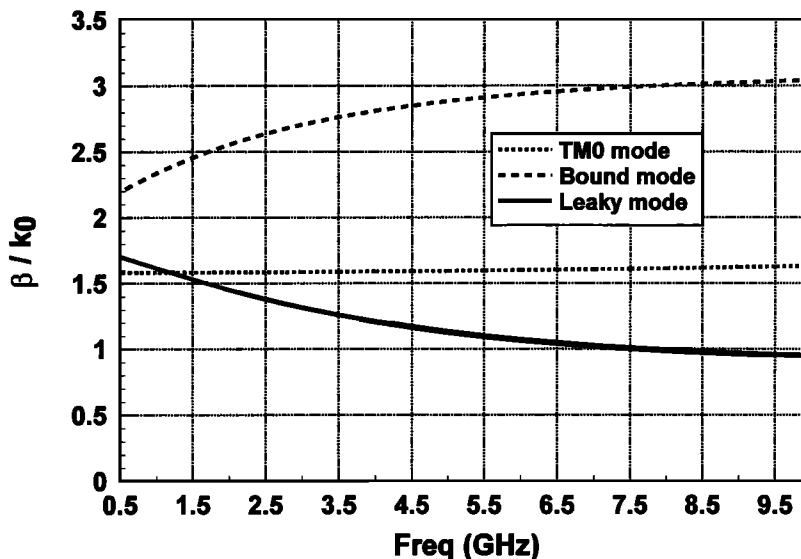


Figure 4. Dispersion plot showing the phase constant of the bound mode, leaky mode, and TM_0 parallel-plate mode versus frequency, for the two-layer stripline structure of Figure 1 with $\epsilon_{r1} = 10.0$, $\epsilon_{r2} = 1.0$, $h_1 = 1.0$ mm, $h_2 = 0.5$ mm, and $w = 7.0$ mm.

in the limit $s \rightarrow 0$, corresponding to $k_x \rightarrow k_{TM_0}$ and $k_{xp} \rightarrow 0$. Therefore, in the spectral-domain analysis, the Fourier transform of the basis functions evaluated at $k_x = 0$ appears (as seen in equation (28), for a single basis function). Evaluating the transform of a basis function at $k_x = 0$ is equivalent to an integration of the function across the strip width (this follows directly from the definition of the Fourier transform). In a complete basis function expansion involving the weighted Chebyshev polynomials, only the lowest-order basis function has a nonzero integral over the strip interval (a nonzero average value). Hence the transform of all higher-order basis functions evaluated at $k_x = 0$ is zero. The result of this is that the higher-order basis functions do not contribute to the leading asymptotic expansion of the residual-wave current. Results will be presented in the next section to verify this interesting feature.

5. Results

Results are shown for the two-layered stripline structure shown in Figure 1, with $\epsilon_{r1} = 10.0$, $\epsilon_{r2} = 1.0$, $h_1 = 1.0$ mm, $h_2 = 0.5$ mm, and $w = 7.0$ mm. The strip is chosen to be wide so that a clear separation occurs between the propagation wavenumbers of the bound

and leaky modes, to make the interpretation of the results easier. (The bound mode is a mode that is a quasi-TEM mode propagating in the high-permittivity region between the strip and the ground plane, while the leaky mode is mainly confined in the air region between the strip and the ground plane.) Results are presented at two different frequencies, 8.0 and 1.0 GHz. At 8.0 GHz a physical leaky mode is present, while at 1.0 GHz there is no physical leaky mode. Unless otherwise indicated, all results have been computed using three longitudinal (z-directed) basis functions and two transverse (x-directed) basis functions for the current profile.

The dispersion curve for the structure in Figure 1 is first shown in Figure 4. The plot is the same as that used by *Di Nallo et al.* [1998] and is reproduced here for convenience. At 8.0 GHz the leaky mode is physical since $\beta_{LM} < k_{TM_0}$ [*Di Nallo et al.*, 1998]. At 1.0 GHz the leaky mode is nonphysical since $\beta_{LM} > k_{TM_0}$. In this region the leaky mode is said to reside in the "spectral-gap" region [*Shigesawa and Oliner*, 1993].

Figure 5 shows a plot of the total strip current and the continuous-spectrum (CS) current produced by the delta-gap source. The total current is found from a numerical evaluation of (1). The CS current is calculated by subtracting the bound-mode current from the total current, with the bound-mode current found from the residue of the bound-mode pole in the k_x

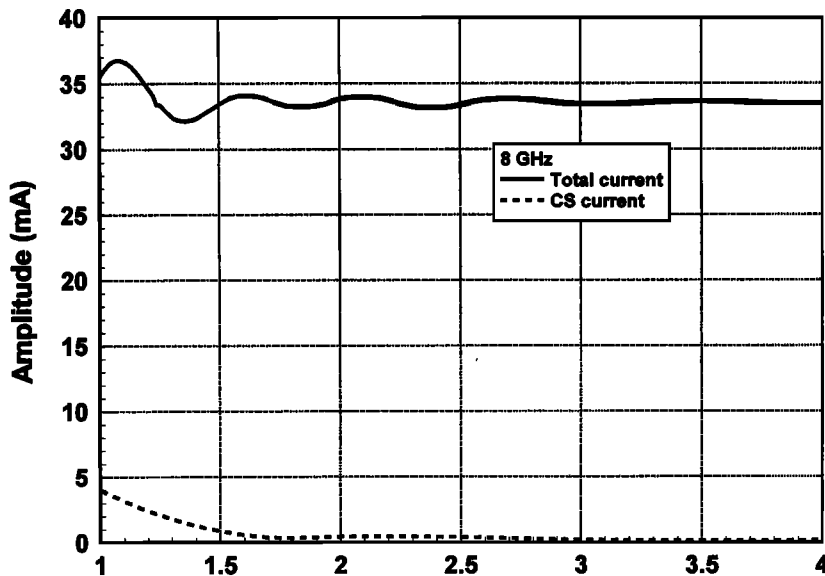


Figure 5. A plot of the total strip current and the continuous-spectrum current (CS) versus normalized distance from the delta-gap source, for the structure of Figure 4 at a frequency of 8.0 GHz.

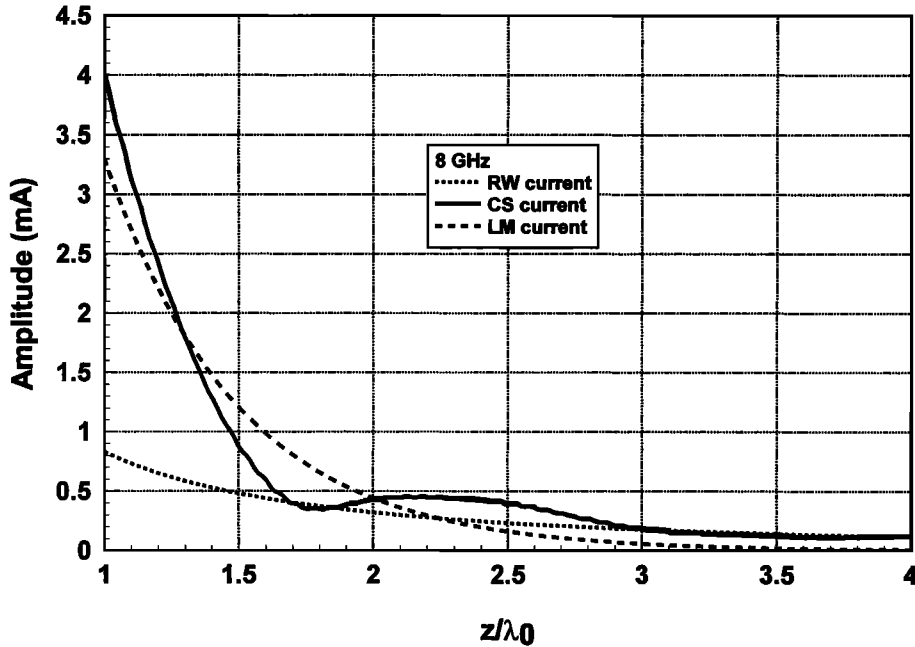


Figure 6. A plot of the continuous-spectrum (CS) current and its constituent parts, the leaky-mode (LM) current and the residual-wave (RW) current, versus normalized distance from the delta-gap source, for the structure of Figure 4 at a frequency of 8.0 GHz.

plane. The oscillations observed in the total current are due to interference between the bound-mode current and the CS current.

Figure 6 shows the CS current replotted on an expanded scale, along with its constituent parts, the leaky-mode (LM) current and the residual-wave (RW) current. The exact RW current shown here is calculated by a numerical integration along the TM_0 SDP. For smaller distances from the source, z/λ_0 less than about 1.5, the CS current is fairly well approximated by the LM current. For larger distances, z/λ_0 greater than about 3.0, the CS current is almost entirely dominated by the RW current since the LM current has decayed to a negligible value.

Figure 7 shows the exact RW current compared with the asymptotic result. The agreement is seen to be excellent for all z/λ_0 greater than about 1.0.

The next set of results are for a frequency of 1.0 GHz. Figure 8 first shows again the total and CS current. In contrast to Figure 5, the oscillations in the total current in Figure 8 do not decay rapidly with increasing distance. This is because there is no physical leaky mode at 1.0 GHz, as seen from the dispersion plot in Figure 4. The oscillations are therefore due to the

interference between the BM current and the RW current, which decays much slower than the LM current in Figure 5.

Figure 9 shows the CS current, which is exactly the same as the RW current since there is no physical LM current at this frequency. In spite of this, a LM current plot is shown in Figure 9. The LM current is obtained from the residue of the LM pole in the k_z plane, even though the LM pole is not captured by the SDP path deformation, and therefore plays no role in the representation of the CS current. The inclusion of the LM current in Figure 9 is presented to verify that when a LM pole is nonphysical, and therefore not included in the mathematical representation of the CS current, the total current does not resemble the current of the leaky mode.

Figure 10 shows the asymptotic RW current from (31) compared with the exact RW current calculated by a numerical integration along the SDP. The "exact" RW current in this figure has been calculated in two ways: using a single basis function of longitudinal current, and using three basis functions of longitudinal current along with two basis functions of transverse current. For large distances from the source, it is seen that the RW current

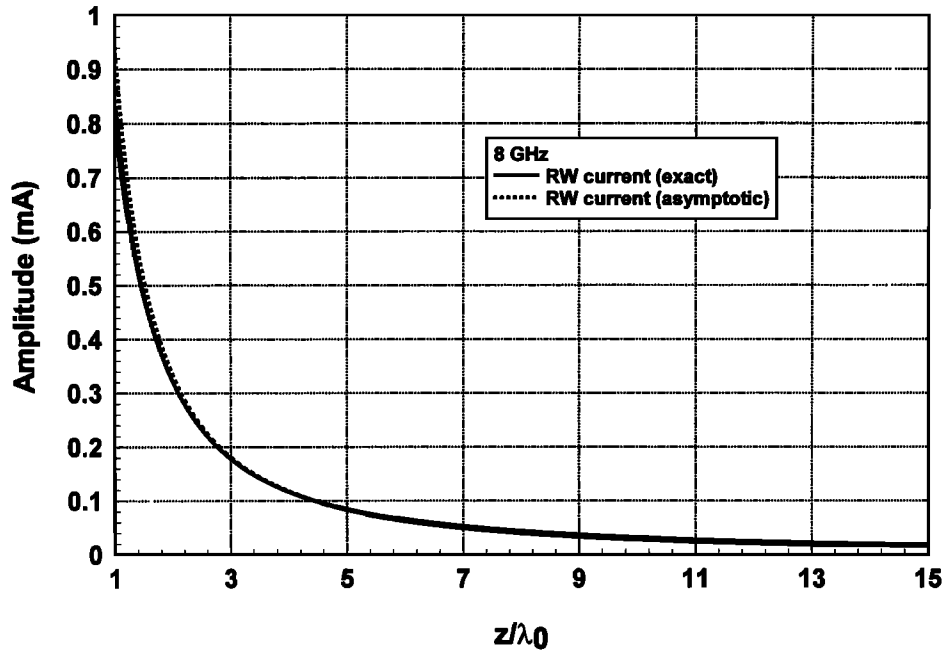


Figure 7. A plot of the exact residual-wave (RW) current and the results from the closed-form asymptotic expression versus normalized distance from the delta-gap source, for the structure of Figure 4 at a frequency of 8.0 GHz.

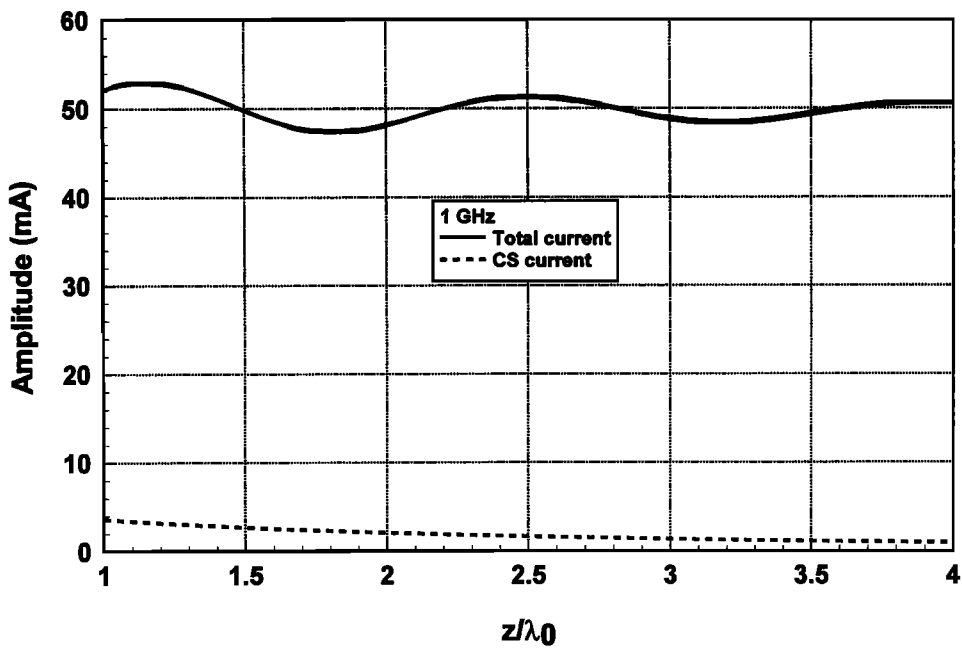


Figure 8. A plot of the total strip current and the continuous-spectrum current (CS) versus normalized distance from the delta-gap source, for the structure of Figure 4 at a frequency of 1.0 GHz.

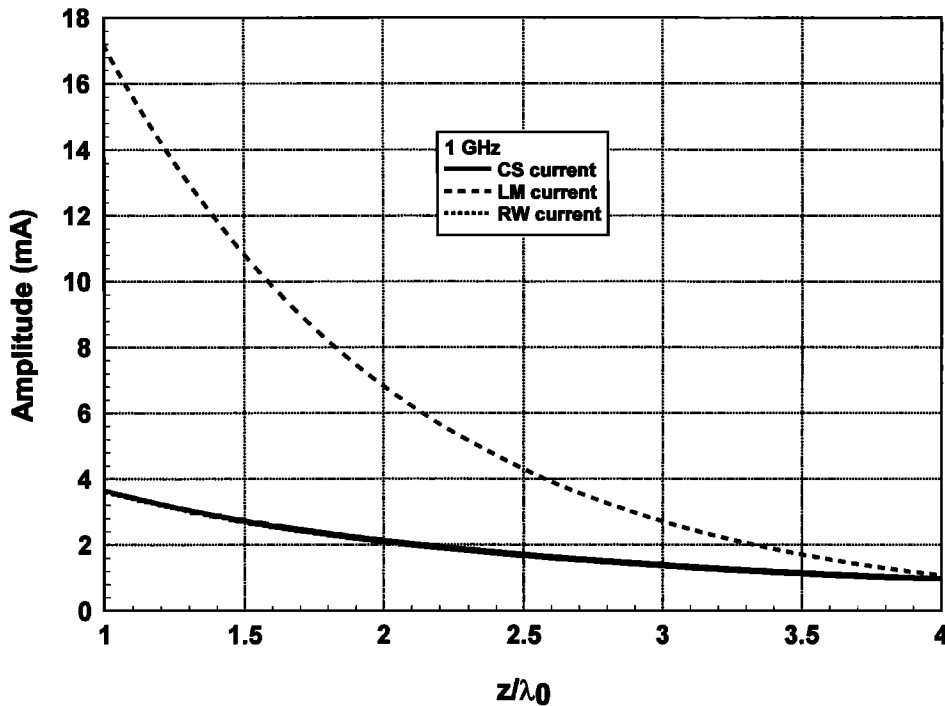


Figure 9. A plot of the continuous-spectrum (CS) current and the residual-wave (RW) current versus normalized distance from the delta-gap source, for the structure of Figure 4 at a frequency of 1.0 GHz. The continuous-spectrum current and the residual-wave current are the same, because there is no physical leaky mode at this frequency. The leaky-mode (LM) curve is a plot of the residue contribution from the leaky-mode pole, even though the pole is not captured by the steepest-descent deformation (the leaky-mode current is therefore not a part of the continuous-spectrum current).

calculated using the single basis function is quite accurate and is asymptotically the same as the result obtained using multiple basis functions. This verifies that the inclusion of high-order basis functions does not affect the asymptotic accuracy of the residual-wave calculation, as expected. The inclusion of higher-order basis functions does improve the residual-wave calculation near the source, however. Comparing with the results shown in Figure 7, it is seen that the residual-wave current reaches its asymptotic form more slowly in Figure 10, where the leaky-mode pole is close to the spectral gap and is hence located close to the SDP path in the k_z plane. The disturbing influence of the pole on the residual-wave current is thus evident and in accordance with the previous discussion regarding the physical interpretation of the leaky-mode and residual-wave currents when a pole is close to an SDP path (and hence close to the spectral-gap boundary).

6. Conclusions

A formulation for the current excited by a delta-gap source on the conducting strip of a general multilayer stripline structure has been presented. The current is calculated in the form of an inverse Fourier transform in the longitudinal (z) direction, corresponding to an integration in the wavenumber variable k_z . The integrand, which is the transform of the current, is given in terms of a spectral integration in the transverse wavenumber (k_x) plane. In the k_z plane, poles appear corresponding to the bound and leaky modes that are launched on the strip by the delta-gap source. In addition to these poles, branch points appear at the locations of the wavenumbers of the parallel-plate modes that exist on the background layered structure. The branch points arise because of the different paths that are possible in the k_z plane when calculating the

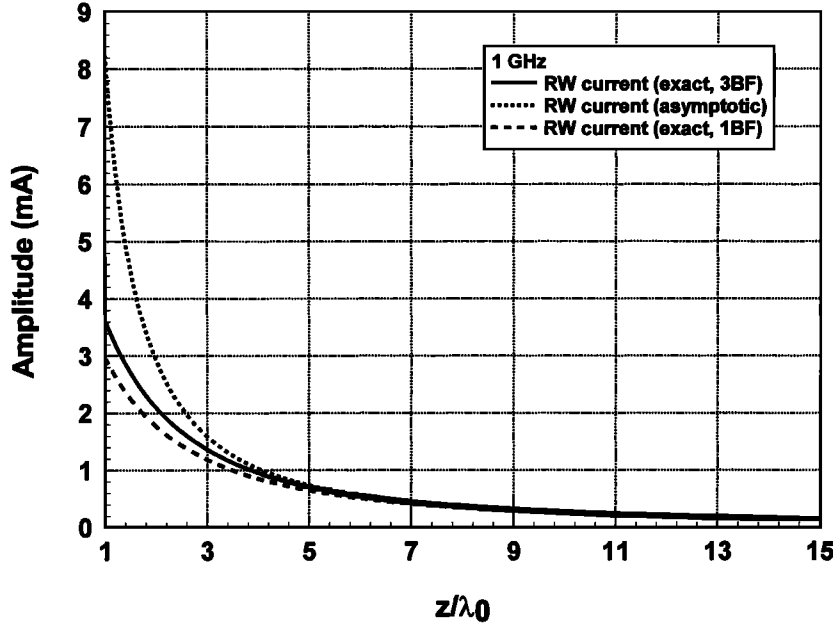


Figure 10. A plot of the exact residual-wave (RW) current and the results from the closed-form asymptotic expression versus normalized distance from the delta-gap source, for the structure of Figure 1 at a frequency of 1.0 GHz. The exact residual-wave current was calculated using both a single basis function and three basis functions to represent the transverse current profile

transform of the current. The branch points play a critical role in the classification and characterization of the strip current excited by the source.

The total strip current is first decomposed into a set of bound-mode currents and a continuous-spectrum current, which is defined as the contribution from an integration around all of the branch cuts. The continuous-spectrum current corresponds physically to radiation from the source into parallel-plate modes. Next, the continuous-spectrum current is further decomposed into a set of physical leaky-mode currents and a set of residual-wave currents. A physical leaky mode is defined here as one that is captured by the deformation of the branch-cut integration into a set of steepest-descent paths, used to asymptotically evaluate the strip current for large distances from the source. The physical leaky modes appear directly in the asymptotic expansion for the continuous-spectrum current on the strip. A residual-wave current is one that propagates with the phase constant of a parallel-plate mode of the background structure and decays algebraically as $z^{-3/2}$. Physically, the residual waves correspond to that portion of the source radiation that is not channeled into

a leaky mode but instead radiates outward directly from the source. Far from the source, after the leaky-mode currents have decayed to a negligible value, the residual-wave currents dominate the continuous-spectrum current.

The residual-wave currents arise from deforming the continuous-spectrum branch-cut integration into the set of steepest-descent paths, each of which surrounds a branch point in the k_z plane. By using an asymptotic analysis, a closed-form expression for the residual-wave currents has been obtained. The results from this asymptotic expression have been compared with an exact calculation of the residual-wave current, and the agreement has been found to be very good, becoming better as the distance along the strip from the source increases.

References

- Abramowitz, M., and I. A. Stegun, *Handbook of Mathematical Functions*, pp. 300-301, Dover, Mineola, N.Y., 1972.
- Bleistein, N., and R. A. Handelsman, *Asymptotic Expansions*

- of *Integrals*, p. 103, Holt Rinehart, and Winston, New York, 1975.
- Chew, W., *Waves and Fields in Inhomogeneous Media*, Van Nostrand Reinhold, New York, 1990.
- Churchill, R. V., *Complex Variables and Applications*, McGraw-Hill, New York, 1960.
- Collin, R. E., *Field Theory of Guided Waves*, McGraw-Hill, New York, 1960.
- Di Nallo, C., F. Mesa, and D. R. Jackson, Excitation of leaky modes on multilayer stripline structures, *IEEE Trans. Microwave Theory Tech.*, **46**, 1062-1071, 1998.
- Jackson, D. R., D. P. Nyquist, F. Mesa, and C. Di Nallo, The role of the steepest-descent path in the excitation of leaky modes on printed-circuit lines, paper presented at the URSI International Symposium on Electromagnetic Theory, Thessaloniki, Greece, May 25-28, 1998.
- Mesa, F., and R. Marqués, Integral representation of spatial Green's function and spectral domain analysis of leaky covered strip-like lines, *IEEE Trans. Microwave Theory Tech.*, **43**, 828-837, 1995.
- Nghiem, D., J. T. Williams, D. R. Jackson, and A. A. Oliner, Proper and improper dominant leaky mode solutions for a stripline with an air gap, *Radio Sci.*, **28**, 1163-1180, 1993.
- Nyquist, D. P., and D. J. Infante, Discrete higher-order leaky-wave modes and the continuous spectrum of stripline, *IEICE Trans.*, **E78-C** (10), 1331-1338, 1995.
- Shigesawa, H., M. Tsuji, and A. A. Oliner, The nature of the spectral gap between bound and leaky solutions when dielectric loss is present in printed-circuit lines, *Radio Sci.*, **28**, 1235-1243, 1993.
- C. Di Nallo, Department of Electronic Engineering, University of Rome "La Sapienza," Via Eudossiana 18, 00184 Rome, Italy.
- M. J. Freire and F. Mesa, Microwave Group, University of Seville, Avd. Reina Mercedes s/n. 41012, Seville, Spain. (mesa@cica.es)
- D. R. Jackson, Department of Electrical and Computer Engineering, University of Houston, Houston, TX 77204-4793. (djackson@uh.edu)
- D. P. Nyquist, Department of Electrical Engineering, Michigan State University, East Lansing, MI 48824. (nyquist@egr.msu.edu)

(Received February 15, 1999; revised July 6, 1999; accepted July 14, 1999.)